

Influence of Aircraft Flow Field on the Longitudinal Stability of a Missile

Konark Arora, Vaibhav Shah, K. Anandhanarayanan,
R. Krishnamurthy, and Debasis Chakraborty*

Defence Research & Development Laboratory, Hyderabad, India

**E-mail: debasis_cfd@drdl.drdo.in*

ABSTRACT

An air-to-air missile launched from a fighter aircraft needs to be stable at launch to enable safe separation from the aircraft, and less stable in the terminal phase of its flight to become highly maneuverable to intercept the targets. A study has been carried out to estimate the effect of the aircraft flow field on the longitudinal stability of the missile using an in-house developed 3-D grid-free Euler solver. Initially, the missiles are placed in the captive location in the launcher of the aircraft. One of the missiles is then moved to various pre-determined locations ahead of the wing of the aircraft, keeping the other missile at the captive location. The centre of pressure and stability margin of the missile is determined at these locations. It is observed that the presence of aircraft has a substantial effect on the longitudinal stability of the missile. The centre of pressure of the missile is seen to move aft as it leaves the launcher. As the missile moves, the centre of pressure reaches a maximum aft position and then moves forward till it reaches a position where the missile is free from the influence of the aircraft. It is observed that as the missile moves away from the region of strong influence of the aircraft, its aerodynamic characteristics approach asymptotically to that of the isolated missile.

Keywords: Grid-free, store separation, chimera cloud, high speed, longitudinal stability

1. INTRODUCTION

The mutual interference of flow fields¹ plays a significant role in determining the performance of the flight vehicles when they are in close proximity to each other. It can enhance or deteriorate the performance of the vehicles flying close to each other. For example, in case of formation flight, the pilots use the advantage of this phenomenon to enhance the performance of their aircraft. At the same time, the wake created by an aircraft in flight can prove fatal to another aircraft closely following it. Hence it is essential to determine the interference effects and their influence on the predicted/ designed performance of the neighbouring vehicles. Till date, the wind tunnel tests, apart from the actual flight tests²⁻⁵ have been the major source of determining the interference effects of various bodies. The actual flight tests, though accurate, are risky and pose a threat to the life of the pilot. The wind tunnel tests on the other hand are quite expensive and time consuming as a significant amount of effort is required to develop a model to account for the fine details of each geometric feature. Another approach is the combination of the wind tunnel and flight tests⁶, which involves determining the differences in the free-stream aerodynamics of the bodies under consideration and then applying these differences to the wind tunnel data. The main assumption in this approach is that the interference effects of these bodies are identical. Recently, computational fluid dynamics (CFD) has been applied to determine the mutual interference

aerodynamics of the bodies^{1,7,8}. CFD based methods are faster as compared to the other methods discussed above. Different numerical methods using potential, Euler and Navier stokes codes have been applied to determine the interference effects of the bodies in flight⁷ and the accuracy of the predicted results improved from potential to Navier stokes calculations. It has also been observed that the Euler simulations are sufficient for predicting the interference effects except in the cases of large flow separation, where Navier stokes simulations are necessary. In this work, the stability of an air-to-air missile in the vicinity of a fighter aircraft is studied using an indigenously developed store separation dynamics suite comprising of a pre-processor, three dimensional Euler solver and a six degree of freedom trajectory program.

2. AIR-TO-AIR MISSILE

An air-to-air missile (AAM) experiences drastic changes in its aerodynamic characteristics as it is under the influence of the aircraft during launch. It is necessary to determine the effect of aircraft flow field on the flight characteristics of the missile. The stability of AAM is one of the main requirements of the AAM for safe separation from the aircraft and it should become less stable in the terminal phase of its flight to meet the maneuvering requirements to out-perform the incoming target, thereby accomplishing its mission successfully. The missile is carried at four locations on the wings of the aircraft (Fig. 1), two on port side and two on starboard side.

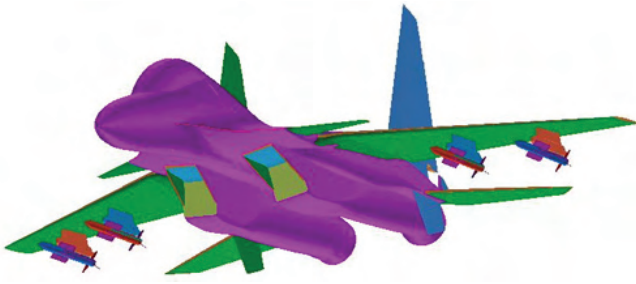


Figure 1. Location of AAM on the aircraft.

The AAM has been designed to be a neutrally stable configuration. It is required to determine the effect of the flow field of the aircraft on the longitudinal stability of the missile so as to determine its ability to fulfill the mission objectives. This has been successfully carried out with the aid of an in-house developed grid-free based CFD code. The movement of centre of pressure and hence the missile stability is expected to be greatly influenced by the presence of the aircraft in its vicinity. As the missile moves ahead of the aircraft, the influence of the aircraft will decrease and the missile is expected to exhibit characteristics similar to that of the isolated missile in regions least influenced by the aircraft flow-field.

A store separation suite⁹ has been developed to predict the separation dynamics of the stores from the aircraft. This suite consists of a grid-free Euler solver, a pre-processor to generate the required data structure for the solver and a 6 degrees of freedom (6-DOF) trajectory solver to predict the store position at successive time intervals. The details of the code and the preprocessor are discussed in the next section. This suite has been validated with the wind tunnel tests of a generic store separating from a wing pylon⁹. The suite uses the quasi-steady approach to simulate the release of the stores from the aircraft. This approach requires the computation of the steady state solution of the governing equations of the fluid flow around the aircraft with the store at each location computed by the 6-DOF solver. However, in the present work, the trajectory of the missile is not determined by the 6-DOF solver. The missile is placed at pre-assigned locations ahead of the wing and the suite is used to determine the pressure field and the location of centre of pressure of the missile at these predetermined locations in the computational domain. The detailed methodology and the results are presented in the following sections.

3. COMPUTATIONAL FLUID DYNAMICS CODE DETAILS

An in-house developed grid-free Euler solver¹⁰ based on entropy variables (q-variables) least squares kinetic upwind method (q-LSKUM)¹¹ has been used to study the effect of the flow field of the aircraft on the static longitudinal stability of the missile. The spatial derivatives in the grid-free Euler solver have been obtained using the least squares method. The grid-free solver, as the name suggests, does not require any grid for the flow simulation, which is an essential requirement for other conventional computational fluid dynamics (CFD) solvers. It instead operates only on an arbitrary point distribution which is extremely easy and fast to generate as compared to grid

generation for a complete complex flight vehicle configuration. The solver uses kinetic schemes and the basic principle behind the kinetic scheme is the fact that the continuum equations of gas dynamics can be obtained as a moment of the Boltzmann equation. The Boltzmann equation in the Eulerian limit (when the collision integral vanishes, the probability distribution function tends to a Maxwellian distribution function):

$$\frac{\partial F}{\partial t} + v_1 \frac{\partial F}{\partial x} + v_2 \frac{\partial F}{\partial y} + v_3 \frac{\partial F}{\partial z} = 0 \quad (1)$$

Here F is the Maxwellian distribution function, v_1 , v_2 and v_3 are the molecular velocity components along the x, y and z directions respectively. Taking ψ moments, we obtain the Euler equations of continuum gas dynamics¹².

$$\frac{\partial U}{\partial t} + \frac{\partial G_1}{\partial x} + \frac{\partial G_2}{\partial y} + \frac{\partial G_3}{\partial z} = 0 \quad (2)$$

where the moment vector $\psi = \left[1, v_1, v_2, v_3, I + \frac{1}{2}(v_1^2 + v_2^2 + v_3^2) \right]^T$, I is the internal energy variable, conserved variable vector $U = \langle \psi, F \rangle$, and the flux vectors are $G_1 = \langle \psi, v_1 F \rangle$, $G_2 = \langle \psi, v_2 F \rangle$, $G_3 = \langle \psi, v_3 F \rangle$. The kinetic flux vector splitting (KFVS) scheme is obtained by splitting Eqn. (1) in CIR split form and then taking ψ moments¹³. The full second order spatial accuracy in the entire domain has been obtained by use of entropy variables and the defect correction method¹⁴. The CFD code has been validated by comparing wind tunnel test results of satellite launch vehicle¹⁰, surface to surface missile¹⁵ and store separation from wings⁹.

In the present work, the point distribution is obtained using overlapped grids. The unstructured grids are generated around the parent aircraft and the missile body separately and are overlapped to form chimera grid. The details of the grid structure and grid independent results are given by Shah¹⁶, *et al.* An efficient preprocessor¹⁷ has been applied to generate the required data structure for the solver using the chimera grids. The preprocessor uses the edge based data structure of the unstructured grids to determine the connectivity for the interior points. The gradient search algorithm¹⁸ is used to determine the neighbours for the nodes in the overlapped region of the chimera grids generated above. An efficient blanking algorithm¹⁸ is used to blank out the points that fall inside the aircraft and the missile bodies. The aircraft has wings, canards and a vertical stabilizer. The missile is an ogive cylinder body with cruciform wings and fins and one set of wire tunnels attached to it. The missile is located at two stations on each side of the wing of the aircraft. The tail fins which are the main control surfaces of the missile are situated in line behind the wings of the missile. The total number of points generated in the computational domain around the aircraft is approximately 3.5 million while the number of points generated in the computational domain around each missile is approximately 2.3 million. The grid around the aircraft is generated by considering only the half geometry, making use of the symmetry of the configuration (Fig. 2). The grid-free solver is applied on these points to determine the aerodynamic loads on the missile. Figure 3 shows the chimera grid around the aircraft and the missiles.

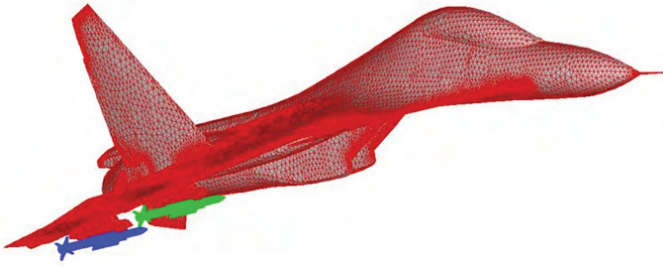


Figure 2. Unstructured surface grid on fighter aircraft with missiles in the captive location.

The right-handed coordinate system has been used for the simulation of separation of missile from the aircraft with the origin at its nose. The anticlockwise moments in the right-handed coordinate system are taken as positive. The positive pitching moment is in the aircraft pitch up direction. The positive rolling moment is in the anti-clockwise direction as viewed from the rear. The positive yawing moment is in the direction of the nose turning towards the port side. The sign convention used is shown in Fig. 4.

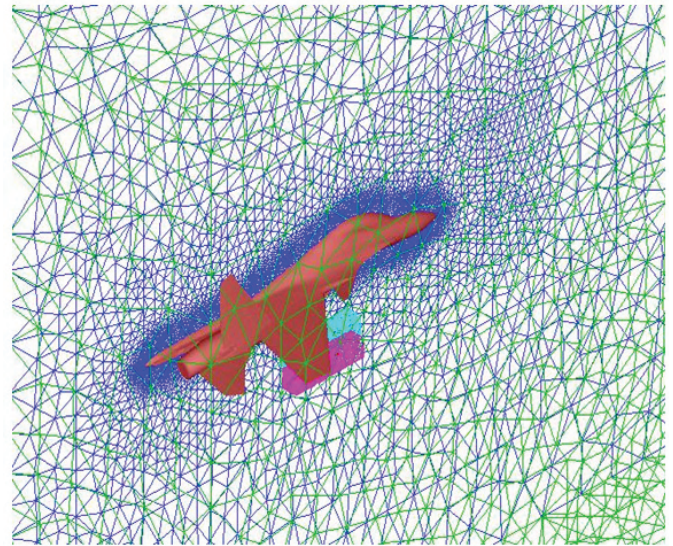


Figure 3. Chimera grid around the fighter aircraft and the missiles.

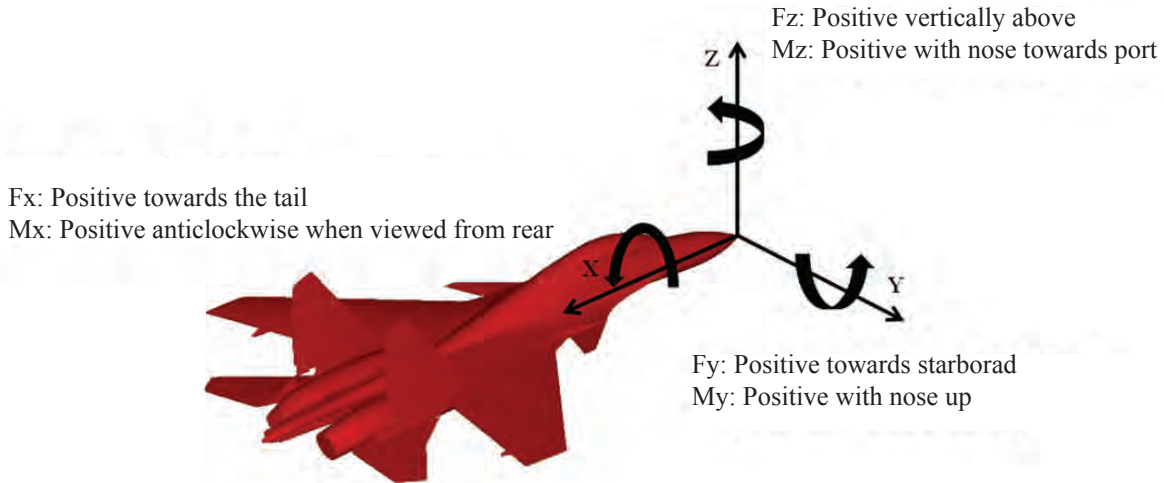


Figure 4. Sign convention for aerodynamic forces and moments.

4. METHODOLOGY

The missiles are placed in the captive location in the launcher of the aircraft. One of the missiles is then moved at various pre-determined locations ahead of the wing of the aircraft, keeping the other missile at the captive location. Table 1 gives the displacement of the inboard and outboard missile (non dimensionalised with missile diameter) from their respective captive locations. Figures. 5(a) and 5(b) show the nine locations of the inboard and the outboard missiles to study the effect of aircraft flow field on the missile characteristics. In these figures, the locations shown as circles correspond to the nose tip of the missile and the location 1 corresponds to the captive location of the missile. The chimera grids (Fig. 3) are generated by overlapping the grids of the aircraft and the missiles at these locations. The preprocessor is used to obtain the chimera point distribution and to generate the data structure required for the grid-free solver. The grid-free solver is applied to simulate the flow field around the missile at these locations in the presence of the parent aircraft at free-stream Mach

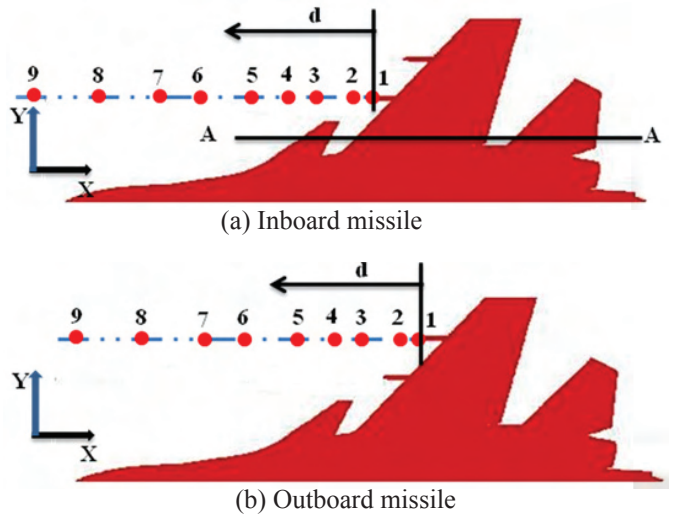


Figure 5. Predetermined location of missile in the presence of the aircraft.

number of 0.6, 0.8, and 1.2 and angle of attack (α) 10° . The forces and moments thus computed by integrating the pressure field around the aircraft and the missiles are used to determine the location of the centre of the pressure. The distance between the centre of gravity of the missile and the location of centre of pressure gives the stability margin of the missile.

5. RESULTS AND DISCUSSION

Figure 6 shows the influence of the aircraft on the pressure field in its vicinity at free-stream Mach number 1.2 and angle of attack (α) 10° . The pressure contours (P/P_∞) are plotted in the pitch plane (XZ plane) of the aircraft (Section Plane AA in Fig. 5). This cross-sectional plane passes through the root section of the wing of the aircraft, cutting the wing, canards and the horizontal stabilizer of the aircraft. The figure shows pressure discontinuities on the canards, wing and the horizontal stabilizer, indicating the presence of strong compression regions near the leading edge of these surfaces. It is observed that the influence of pressure field extends up to a large distance from the vicinity of the aircraft into the computational domain, indicating a strong effect of the aircraft on the pressure field in its neighbourhood. Table 1 shows predetermined location of the nose of in board and out board missiles.

Table 1. Predetermined location of the nose of inboard and outboard missiles.

Displacement from captive location/missile diameter	
Inboard missile	Outboard missile
0.0 (Captive)	0.0 (Captive)
5.62	5.62
16.85	16.85
22.47	22.47
33.71	33.71
44.94	44.94
56.18	56.18
73.03	73.03
89.89	89.89

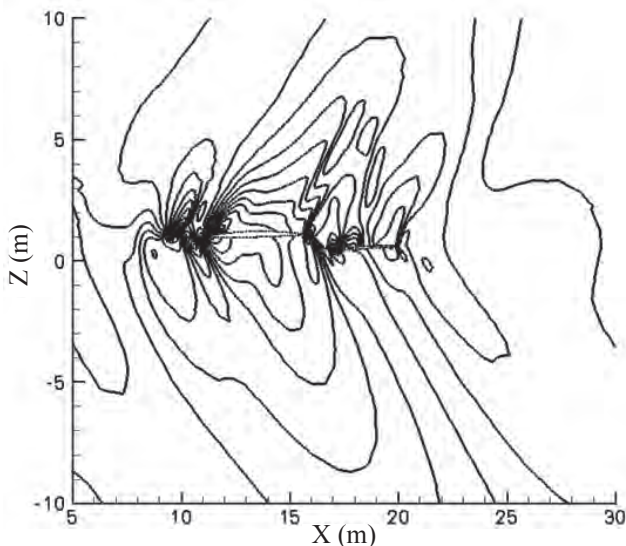


Figure 6. Pressure contours in the plane (AA) that passes through wing root of the aircraft

The surface pressure contours (P/P_∞) on the aircraft with the inboard and outboard missiles placed at above mentioned locations in the computational domain at free-stream Mach number of 1.2 and an angle of attack 10° are shown in Figs. 7(a) and 7(b). A small region of high pressure is observed near the nose and canopy of the aircraft. The surface pressure contours also show that a normal shock appears on the horizontal stabilizer of the aircraft. Due to high angle of attack, the flow expands over the wing of the aircraft. A region of high pressure (a strong compression front) appears near the wing root section of the aircraft and a strong cross flow occurs over the wing surface from the wing root to the wing tip due to highly swept back wing.

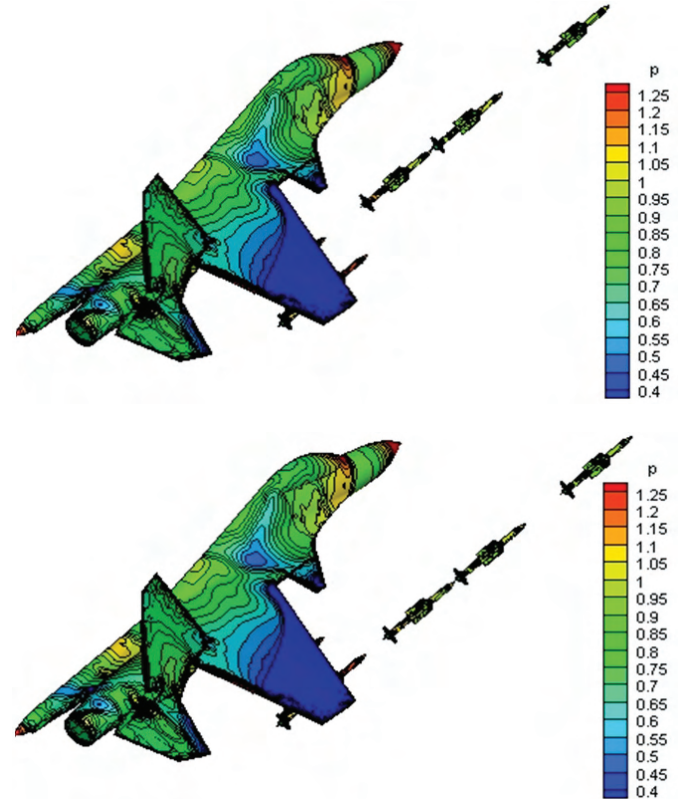


Figure 7. Surface pressure contours on the aircraft and the missiles (a) Inboard missile at different locations (b) Outboard missile at different locations.

The locations of the centre of gravity and the centre of pressure of the missile vary with time. The consumption of the propellant of the missile results in the change in the position of centre of gravity of the missile with time. At the same time, the missile is crossing a region of varying influence of the flow field of the aircraft. This causes a movement of the centre of pressure of the missile, depending upon the location of the missile with respect to the aircraft. The centre of gravity and the centre of pressure are the main parameters which affect the stability of the missile. Thus, the movement of the centre of gravity as well as the centre of pressure of the missile results in the variation of the stability margin of the missile as it leaves the aircraft. A typical case of movement of centre of pressure of the inboard missile at free-stream Mach number 1.2 and $\alpha=10^\circ$, as it is placed at various locations, is analysed here.

The surface pressure distribution on the leeward and the windward side of the inboard missile at various displacements (d) from the captive location of the missile (non dimensionalised with missile diameter) are shown in Figs. 8(a) to 8(f). As discussed earlier, the missile is having an ogive cylinder body, with the launch shoes located on the leeward side of the missile. The flow continuously expands over the ogive nose of the missile, which is indicated by the continuous decrease in pressure on the leeward and windward side of the nose of the missile (Figs. 8(a) to 8(f)). There is a sudden drop in pressure in the ogive-cylinder junction indicating a strong expansion in the region. Discontinuities in the pressure distribution are observed at the location of the launch shoes (at $X/D \sim 9.8, 14.4, 16.2$) on the leeward side of the missile. The pressure distribution over the missile surface shows that the nose ($X/D < 5$), wings ($10.4 < X/D < 14.3$) and tail ($20.2 < X/D < 21.4$) are the major lift producing components.

At the captive location, an upward force is acting in the nose region of the missile, indicated by the net positive pressure difference over the nose (Fig.8(a)). Downstream of the nose, a net negative pressure difference is observed over the missile surface till the location of the wings. The region of positive pressure difference is observed at the tail of the missile. This causes the centre of pressure of the missile to be aft of the centre of gravity of the missile at the captive location. As the missile moves ahead of the captive location

($d = 5.62$, Fig. 8(b)), we observe that the wing of the missile is having a net positive pressure difference compared to the tail region causing a forward shift of the centre of pressure of the missile at this location. Fig. 8(c) shows the surface pressure distribution on the leeward and windward side of the missile located at a displacement of 22.47 from the captive location. At this location, a net positive pressure difference exists at the tail region of the missile also. This results in the centre of pressure to shift aftwards as compared to the previous missile location ($d = 5.62$) discussed above. Comparing the pressure distribution over the missile at a displacement (d) of 22.47 (Fig. 8(c)) and 33.71 (Fig. 8(d)), we observe that there is a reduction in the pressure difference in the tail region when d is 33.71 and this causes the centre of pressure to shift forward. Figs. 8(e) and 8(f) show the surface pressure distribution on the leeward and windward side of the missile for $d = 73.03$ and 89.89, respectively. Here, the nose of the missile is located ahead of the nose of the aircraft. It is observed that at these locations, there is a slight reduction in the net pressure distribution in the tail as compared to the location shown in Fig. 8(d) above. This causes a slight forward shift in the centre of pressure of the missile at these locations in the trajectory. It is observed that as the missile moves away from the influence of the aircraft, the pressure distribution on the missile asymptotically approaches to that of the isolated missile where it is completely free from the influence of the aircraft.

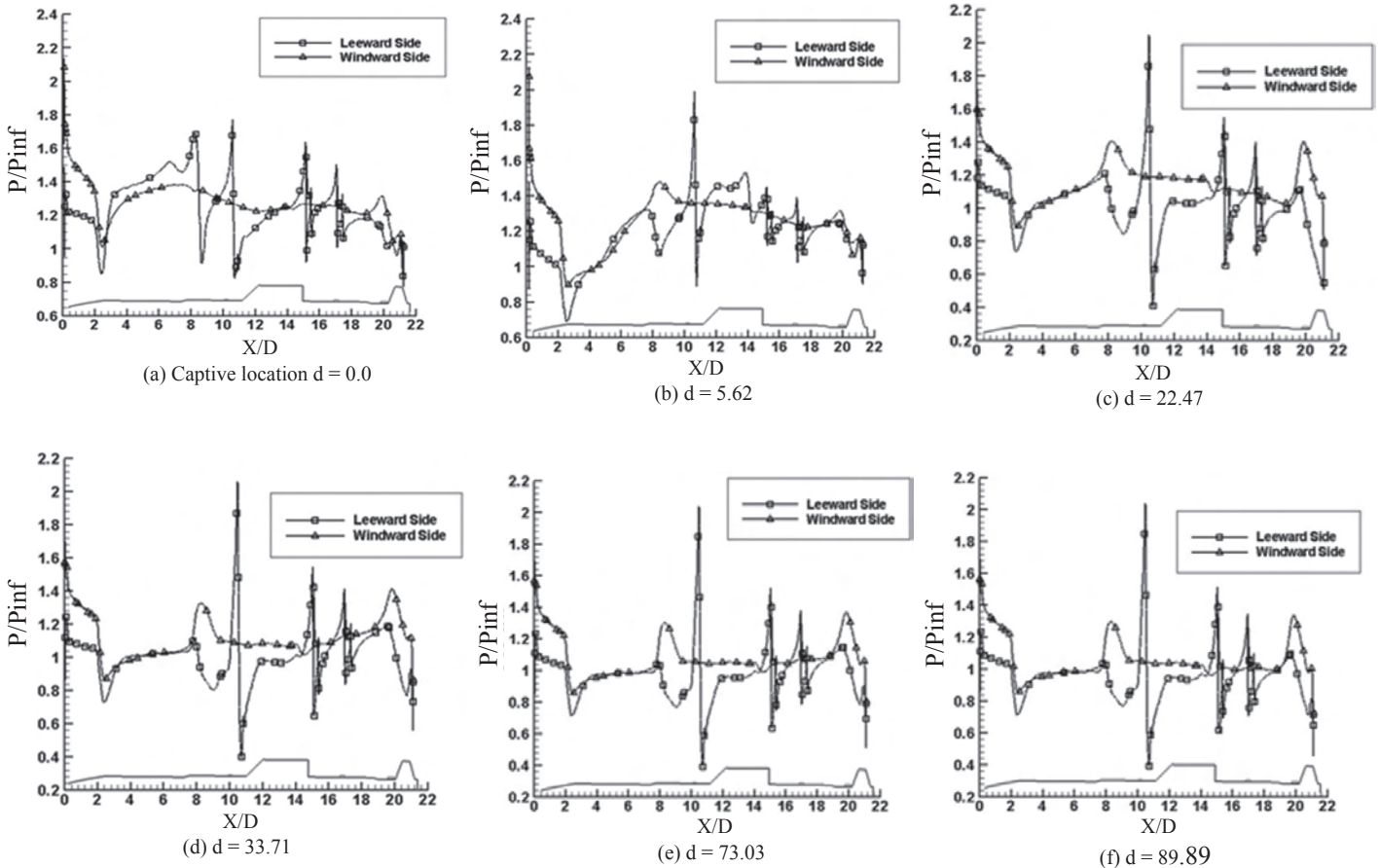


Figure 8. Pressure distribution on leeward and windward side of inboard missile ($M = 1.2, \alpha = 10^\circ$).

The movement of centre of pressure of both inboard and outboard missiles with displacement from the captive location (X/D) along the missile body is shown in Figs. 9(a) and 9(b). It is observed that the centre of pressure of the missile in the captive location is aft of the centre of gravity of the missile and the missile is highly stable at the captive location. Then, as the missile separates, the centre of pressure moves forward making the missile unstable in the launch phase. As the missile clears the launcher of the aircraft, the centre of pressure moves aft of the centre of gravity, reaches to a maximum aft location and then moves forward as tail of the missile crosses the wing leading edge till it asymptotically approaches to the location of centre of pressure of the isolated missile. This observation is consistent with the surface pressure distribution (Fig. 8) obtained on the missile at these pre-determined locations. It is observed that as the missile moves in the regions away from the influence of the aircraft, the pressure distribution on the missile approaches to that of the isolated missile. A similar trend is observed in the movement of centre of pressure of both inboard and outboard missiles at other flow conditions as well.

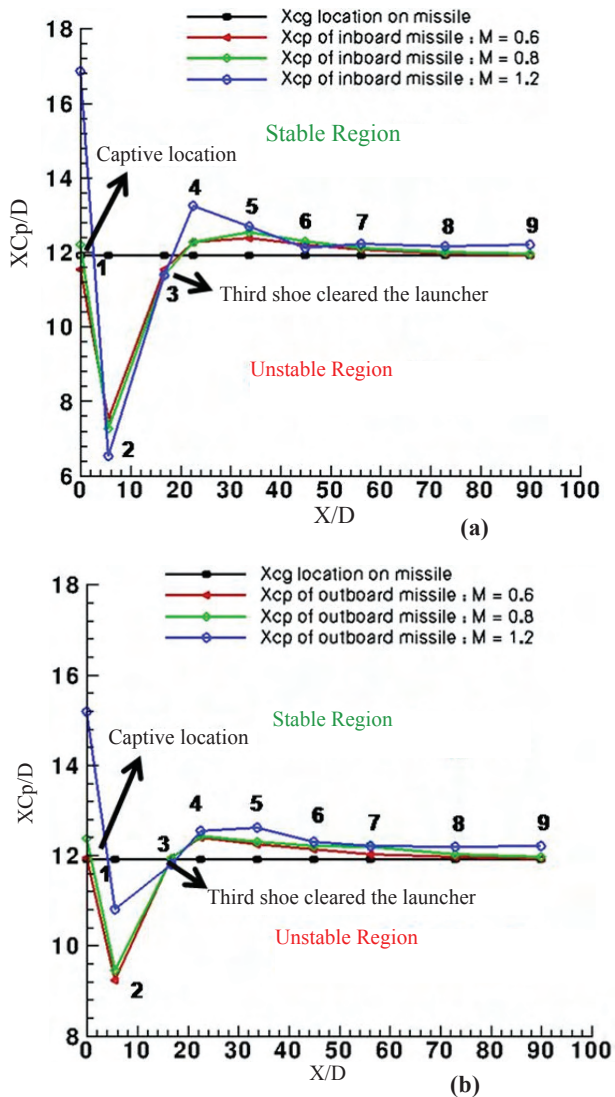


Figure 9. Movement of the centre of pressure of missile along its body, (a) inboard missile and (b) outboard missile.

6. CONCLUSIONS

The effect of the flow field of the parent aircraft on the longitudinal stability of the missile has been studied. The static longitudinal stability of the missile and the location of its centre of pressure at various locations ahead of the aircraft wing were determined using a grid-free solver. The steady state solution of the governing equations of fluid flow around the aircraft, with the missile at the predetermined locations, is found and the location of centre of pressure of the missile and stability margin is determined. It is observed that the static margin of the missile under the influence of the parent aircraft decreases initially as it leaves the launcher of the aircraft. The stability margin of the missile reaches a maximum value, and then again decreases, approaching asymptotically to that of the isolated missile as it moves away from the region of influence of the aircraft.

REFERENCES

1. Kern, S.B. & Findlay, D.B. F/A-18C store carriage loads prediction and mutual interference aerodynamics. *In the RTO SCI Symposium on Aircraft Weapon System Compatibility and Integration*. Chester, United Kingdom, 28-30 September 1998, RTO MP-16.
2. Hong Kim, Ji; Hyeon Sohn, Chang & Lee, Ilwoo. T-50/A-50 FSD stores separation program. AIAA Paper 2006-6000, 2006.
3. Cenko, A.; Lee, J.; Getson, E.; Hallberg, E.; Jolly, B. & Sickles, W. IHAAA applications to reducing store separation flight testing. AIAA Paper 2007-1653, 2007.
4. Hong Kim, Ji; Lee, Ilwoo & Don Yang, Hee. Integrated test and evaluation approach to improve aircraft store separation. AIAA Paper 2005-6223, 2005.
5. Hallberg, E.; Ray, E. & Fitzwater, R. Store separation trajectory simulation for the high speed anti-radiation demonstrator (HSAD) program. AIAA Paper 2006-460, 2006.
6. Findlay, David B. Aero loads prediction of a fuselage mounted store on the F/A-18C. AIAA Paper 95-0040, 1995.
7. Kern, S.; Hoffman, L. & Moyer, S. Free-stream and captive potential, Euler and Navier-Stokes simulations of the AGM-84 and GBU-24 on the F/A-18C. AIAA Paper 94-0053, 1994.
8. Jeter, Edward L. Applications of modern multidisciplinary approaches to the integration of weapons on aircraft. *In the RTO Symposium on Aircraft Weapon System Compatibility and Integration*. Chester, United Kingdom, 28-30 September, 1998, RTO MP-16.
9. Harish, G.; Pavankumar, M. & Anandhanarayanan, K. store separation dynamics using grid-free Euler solver. AIAA Paper 2006-3650, 2006.
10. Anandhanarayanan K.; Nagarathinam, M. & Deshpande, S.M. Development and applications of a grid-free kinetic upwind solver to multi-body configurations. AIAA Paper 2005-4846, 2005.
11. Deshpande, S.M., Anandhanarayanan, K., Praveen, C. & Ramesh, V. Theory and application of 3-D LSKUM based on entropy variables. *Int. J. Numer. Meth. Fluids*, 2002,

40(1-2), 47-62

12. Deshpande, S.M. Kinetic theory based new upwind methods for inviscid compressible flows. *AIAA Paper* 86-0275, 1986.
13. Mandal, J.C. & Deshpande, S.M. Kinetic flux vector splitting for Euler equations. *Comp. Fluids J.*, 1994, **23**(2), 447-478.
14. Dauhoo, M.Z.; Ghosh, A.K.; Ramesh, V. & Deshpande, S.M. q-LSKUM – A new high order kinetic upwind method for Euler equations using entropy variables. *In the 8th International Symposium on Computational Fluid Dynamics, Bremen, Germany, September 5-10, 1999.*
15. Anandhanarayanan, K.; Shah, Vaibhav; Krishnamurthy, R. & Debasis, Chakraborty. Numerical exploration of an aerospace vehicle with deflected fins using a grid-free solver. *In the Proceedings of SAROD-2007, Thiruvananthapuram, 22-23 November 2007, 536-544.*
16. Shah, Vaibhav; More, R.R.; Srinivasa Raju, S.; Anandhanarayanan, K.; Krishnamurthy, R. & Debasis, Chakraborty. Estimation of captive flight loads using grid-free Euler solver. *Journal Aircraft*, **48** (4), 2011, 1273-1279.
17. More, R.R.; Srinivasa Raju, S.; Anandhanarayanan, K. & Krishnamurthy, R. Nose panel opening study of a hypersonic launch vehicle. *In the Proceedings of the first International Conference on High Speed Transatmospheric Air & Space Transportation, Hyderabad, India, June 2007, pp.171-177.*
18. Meakin, R.L. Composite overset structured grids. *In the Handbook of Grid Generation, edited by Thompson, J.F.; Weatherill, N.P. & Soni, B., 1999, pp. 11.1 – 11.20.*

Contributors



and meshless methods.

Dr Konark Arora obtained his PhD (Aerospace Eng.) from Indian Institute of Science (IISc), Bengaluru, in 2007. Currently working he in Computational Fluid Dynamics (CFD) Division, DOCD, Defence Research and Development Laboratory (DRDL), Hyderabad. His areas of interest includes: Computational fluid dynamics, aerodynamics, kinetic schemes



Mr Vaibhav Shah received his BTech (Mechanical Eng.) from REC, Kurukshetra in 2002. He is working in the DRDL, Hyderabad since 2004. He has 2 journal and 5 conference publications to his credit. His areas of interests include: Code development for CFD applications, structured/unstructured grid-generation and CFD flow simulation over missiles.



solver for non-equilibrium transitional flows and distributed computing.

Dr K. Anandhanarayanan received his PhD (Aerospace Eng.) from IISc, Bengaluru. He is working in the DRDL, Hyderabad since 1993. He has 10 journal and 45 conference publications to his credit. His areas of interests include: Algorithm development for CFD applications, grid-free Euler and Navier-stokes solvers, direct simulation monte carlo based Euler-Boltzmann coupled



Roy Trust Award – 1991, DRDO Technology Award – 1994 and DRDL Technology Award – 2008. He is a Fellow of The Institution of Engineers (India) and council member of the AP State Centre of IEI.

Dr R. Krishnamurthy received his PhD (Aerospace Eng.) from IISc, Bengaluru. Presently heading the CFD Division IN DRDL, Hyderabad. He has developed indigenously advanced CFD solvers and grid generators for simulating steady and unsteady flows for missile aerodynamics. He has published more than 50 technical papers. He is a recipient of *Dr Biren*



and propulsion.

Dr Debasis Chakraborty obtained his PhD (Aerospace Eng.) from IISc, Bengaluru. Presently, he is working as Technology Director, Computational Dynamics, DRDL, Hyderabad. He has about 48 journal and 58 conference publications to his credit. His research interests include: CFD, aerodynamics, high speed combustion